DESIGN OF DYNAMIC COMPENSATION SYSTEM FOR CORN SEEDING POSITION BASED ON FUZZY PID CONTROL AND ANALYSIS OF BENCH TEST
/
玉米播种位置动态补偿系统设计与台架试验分析

Kaikang CHEN [1,2], Yanwei YUAN [2], Bo ZHAO [2], Liming ZHOU [2], Kang NIU [2], Xin DONG [2], Xin JIN [3], Yongjun ZHENG [1*]

[1] College of Engineering, China Agricultural University, Beijing, 100089, China;
[2] The State Key Laboratory of Soil, Plant and Machine System Technology, Chinese Academy of Agricultural Mechanization Sciences, Beijing, 100083 China;
[3] College of Agricultural Equipment Engineering, Henan University of Science and Technology, Luoyang 471003, China.
E-mail: zyj@cau.edu.cn
DOI: https://doi.org/10.35633/inmateh-67-40

Keywords: *Corn; Planting distance; Row spacing; Sowing place; The sensor; Dynamic compensation; Fuzzy PID control*

ABSTRACT
Aiming at the problem that the existing planters cannot accurately maintain the seeding spacing and row spacing in the field, the high-speed photography technology is used to analyze the seeding trajectory, so as to determine the key factors affecting the seeding position. First, a dynamic compensation system for maize seeding position based on fuzzy PID control was designed. In the dynamic compensation system, the biaxial angle sensor was used to detect the angle of seeding monomer, and the space rotation theory was used to calculate the offset of the seeding position. Then, the dynamic compensation of seeding position was completed by the fuzzy PID control servo electric push rod, and the response time of fuzzy PID control system was 0.035 s. When the seed spacing of maize was 30 cm, the conveyor speed was 1.67 m/s and the seed tray speed was 30 r/min. Finally, the bench test was carried out under the conditions of random disturbance signal, sinusoidal wave disturbance signal and random disturbance signal plus sinusoidal wave disturbance signal. The results showed that compared without dynamic compensation, the variation coefficient of the longitudinal grain spacing and the transverse grain spacing decreased by an average of 6.94 % and 9.16 %, respectively. In this way, this study can provide a reference for improving the stability of seeding row spacing and plant spacing.

摘要
针对现有播种机田间作业时无法精确保持播种株距和行距的问题，通过高速摄影技术对落种轨迹进行分析，确定了影响播种位置的关键因素，设计了基于模糊 PID 控制的玉米播种位置动态补偿系统。动态补偿系统主要包括六自由度平台、播种单体、动态补偿机构、双轴倾角传感器和工控机组成。它采用双轴倾角传感器检测播种单体的倾角变化，通过空间旋转理论计算播种位置的偏移量，然后通过模糊 PID 控制伺服电动推杆完成播种位置动态补偿，模糊 PID 控制系统的响应时间为 0.035 s。当玉米播种粒距为 30 cm、传送带速度 1.67 m/s、排种盘转速 30 r/min 时，在随机扰动信号、正弦波扰动信号和随机扰动信号加正弦波扰动信号情况下进行台架试验。试验结果表明：与未使用动态补偿功能相比，使用动态补偿功能时的纵向粒距变异系数平均降低了 6.94 %，横向粒距变异系数平均降低 9.16 %，实现播种位置动态补偿。该研究为提高播种行距和株距的质量提供了借鉴。

INTRODUCTION
According to the requirements of modern agronomy, the precise positioning seeding of maize is a technology in which the maize seeds are planted in the soil at fixed points and quantitatively seeded according to the precise row spacing, plant spacing and sowing depth.

*Chen Kaikang, Ph.D. Stud.; Yuan Yanwei, Researcher, Ph.D.;ZhaoBo, Researcher, Ph.D.; Zhou Liming, Researcher, Ph.D.; Niu Kang, Senior engineer; Dong Xin, Senior engineer; Jin Xin, Associate Professor, ZhengYongjun *, Prof. Ph.D.*

Compared with precise seeding, the position of maize seeds in the soil was emphasized *(Ji et al., 2021; Poncet et al., 2018; Huang et al., 2016)*. The value of precise positioning and seeding lies not only in saving seeds and reducing costs, but also in improving the quality of seeding, making seedlings orderly, improving the utilization rate of light energy and soil power, and providing highly consistent operating objects for the mid-term management and harvesting, to effectively improve the yield per unit area *(Liu et al., 2017; Huang, 2015; Liu, 2013).*

In the actual planting, affected by the factors such as uneven ground and stubble cover, the single seed row is easy to tilt and shift. This is easy to change the seed row spacing and plant spacing, reduce the sowing quality, and affect the yield per unit area of maize *(Wiggans 1939; Joseph and Mike, 2014; Moore1991).* As such, the United States Precision Planting Company optimized the structure of the finger-clamp seed metering device to make the seeds are always in the center of the seed guide belt. At the same time, a buffer pad is set at the entrance to reduce the collision and rebound in the seed metering device, as well as the changes of plant spacing and row spacing *(Precision 2016).* Precision Planting, an American company, created a belt seeding device called Speed Tube. It uses a pair of seeding wheels with opposite directions to pull seeds into separate compartments on the conveyor belt. As the belt moves down to the bottom, it drops into the seed bed at a lower height. In the whole process, the seed metering device provides a uniform flow of seeds, and the seed turntable transports the seeds to the conveyor belt for segmentation. The rotation speed of the conveyor belt controls the seed spacing *(Yang et al., 2015; Chen et al., 2018)*.

The Swedish Vaderstad company matched a pressurized seed metering device for the high-speed planter, which uses pneumatic projection technology to control the trajectory of planting to achieve precise planting. This dropping method can reduce the collision between the seed and the seed metering tube, and improve the accuracy of seed dropping. *Yazgi, (2016),* analyzed the effect of different shapes of seeding tubes on seed spacing uniformity, and found that the seed spacing uniformity of the best and worst seeding tubes was 85.6% and 67.2%, respectively. (*Zhao et al., 2018)*. In the suppression, the magnitude of the ballast pressure needs to be carefully considered. If the ballast pressure is too high, the seeds may be directly pressed into the soil, hardening the soil layer, which is not conducive to the development of seeds; on the contrary, the seeds will not be pressed *(Sivarajan et al., 2018).* Bahauddin Zakariya University *(Ahmad et al., 2021)* studied the influence of the bed pneumatic corn planter at three tillage levels and four sowing operation speeds. The results showed that the bed pneumatic corn planter can accurately sow within the error range.

Karimi et al., (2019), designed a new seeder monitoring system based on the infrared sensor. He sensed the seed flow through the infrared sensor, measured the ground speed through the hall sensor, and calculated the actual sowing rate according to the sowing rate per unit area. *Xie et al. (2021)* designed a method for seeding parameter monitoring based on a laser sensor. In a dusty environment, the monitoring accuracy of the laser sensor was higher than that of the photoelectric sensor, and the seeding parameters were more accurate. At the speed of 5, 6, 7, 8 and 9 km/h, the average error of each monitoring parameter of the laser sensor was less than 0.5%. The test showed that the laser sensor was more reliable than the photoelectric sensor. *Yin, (2014),* discussed the seeding monitoring, fertilization monitoring and bellows pressure monitoring, and designed an intelligent monitoring system. Compared with previous monitoring systems, this system mainly adopts modular, high-sensitivity sensors and wireless transmission technology, which is easy to maintain and has high reliability.

In the previous studies, the structure of seed metering device and seed metering tube was usually optimized or monitored to maintain good plant spacing and row spacing. However, in a complex field environment, uneven ground often caused great changes in the outlet of the seed metering tube, resulting in poor consistency of plant spacing and row spacing *(Xia et al., 2011).*

Through the study of the sowing trajectory, the main factors affecting the seeding position were analyzed, and a dynamic compensation system for maize seeding position based on fuzzy PID control was designed. In the system, a biaxial tilt sensor was used to measure the dip angle of the seeding unit, and the offset of the seeding position was calculated by the space rotation theory. Then the position of the seeding tube was adjusted through the fuzzy PID control servo electric push rod. The dynamic compensation of the seeding position was completed and the stability of plant spacing and row spacing was maintained.

MATERIALS AND METHODS

According to the actual working conditions in the field, the main factors that affect the seed dropping position are the speed of the seed metering device, the position of the seeding tube and the inclination angle

of the metering device. In this paper, the influence of these three factors on seed dropping position was analyzed experimentally.

The corn seed variety used in the experiment was Zhengdan958, with a mass of 304.26 g per thousand grains and an average density of 1.10 g/cm3. The average geometric size was 11.06×8.38×4.03 (mm, length × width × thickness), and the average water content of 100 seeds was 11.2%~13.1%.

The seeding experiment was completed with a high-speed photographic system and a seeding performance test bed. Through the seeding performance test bench, the rotation speed of the seed meter, the position of the seeding tube and the inclination angle of the seed meter were changed. The seed trajectory of the seed from the outlet of the seeding tube to the conveyor belt was collected through high-speed photography, and the falling motion law of the seed was analyzed.

High-speed camera system includes the Phantom high-speed camera, fill light and computer. The equipment parameters are shown in Table 1.

Table 1

Equipment parameters required for the test

Equipment	Type	Parameter	Value	Manufacturer
High speed camera	Phantom M110	Resolution/px	1920×1200	VRI, Inc
		Maximum shooting speed/FPS	1800	
Fill light	PhantomM110	Output power /W	100	VRI, Inc
Computer	FX506	Hard disk capacity /T	1	Asus
		Run memory /G	8	

During the test, the position of the seed drainer and the flexible seed drain pipe were fixed. Through the control software of the seeding performance test bench, the speed of the seed meter, the position of the seed tube and the tilt angle of the seed meter were adjusted. After entering a stable seeding stage, a high-speed camera was used to record the falling process of seeds, as shown in Figure 1. Hydraulic oil was applied on the conveyor belt of seed bed to prevent the seed from bouncing due to the excessive landing speed.

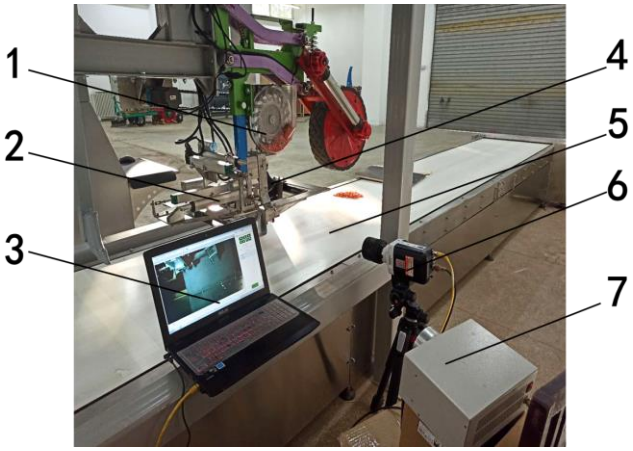

Fig. 1 - Composition of seeding test system

1. Seed metering device; 2. Dynamic compensation mechanism; 3. Computer; 4. Seeding tube; 5. Conveyor belt; 6. High-speed camera 7. Fill light;

In the experiment, the point projected on the conveyor belt in the vertical position of the seed tube and the outlet of the seed metering device was taken as the origin O. The movement direction of the conveyor belt was set as the positive x-axis (longitudinal) to determine the positive y-axis (lateral) according to Descartes' right-hand rule.

After the high-speed photography was completed, the measurement function of Phantom software system was used to track the movement track of maize seeds in the video, and the seed falling track was analyzed. The test results refer to GB/T 6973-2005 "Single (precision) seeder test method", and the longitudinal grain distance coefficient of variation (x-axis) and transverse grain distance coefficient of variation (y-axis) were examined.

According to the above analysis, there are two main reasons for the deviation of seed dropping position: One is that the speed of the seed metering device changes drastically and the other is that the position of the seeding tube and the inclination angle of the seed metering device change simultaneously. When working in the field, the rotation speed of the seed metering device is basically unchanged.

Therefore, the dynamic compensation system for the seeding position designed in this paper is mainly to reduce the influence of the planting position change on the plant spacing and row spacing caused by the simultaneous change of the inclination angle of the seed metering device and the position of the seeding tube.

- **CALCULATE THE OFFSET OF PLANTING POSITION**

During the field sowing, the unevenness of the ground caused the monomer to tilt to change the sowing position. In this paper, the biaxial tilt sensor is used to detect the tilt change of the seeding monomer, and the motion of compensation mechanism is linear in x and y directions. Therefore, it is necessary to convert the change of the inclination angle of the seed metering device into the linear offset of the outlet of seeding tube.

The controlling property of the seeding position in three-dimensional space is that the rotation of the plane of the two-dimensional coordinate system rotates around a fixed axis. Therefore, in order to analyze the rotation law of the planting position in three-dimensional space coordinates, a three-dimensional space coordinate system of the planting position is established, as shown in Figure2.

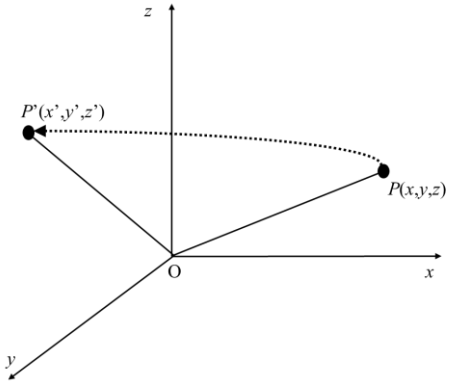

Fig. 2 - Three-dimensional spatial coordinate rotation map

Note: P is the initial position of the seed metering tube, and P′ is the position of the seeding tube after rotation

The rotation of points in three-dimensional space can be regarded as the rotation of points in two-dimensional space (xOy, xOz, yOz) around the axis (x axis, y axis, and z axis). During the rotation of plane xOy around the z-axis, the coordinate value z of point P remained unchanged. Similarly, the coordinate value on the x-axis remained unchanged when the point P rotated around the x-axis. The coordinate value on the y-axis remained unchanged when the point P rotated around the y-axis. According to the above analysis, point P rotates counterclockwise around the x axis, the rotation matrix obtained when the rotation angle α is:

$$R_\alpha = \begin{pmatrix} 1 & 0 & 0 \\ 0 & \cos\alpha & \sin\alpha \\ 0 & -\sin\alpha & \cos\alpha \end{pmatrix} \quad (1)$$

Point P rotates counterclockwise around the y-axis, and the rotation matrix obtained by the rotation angle β is:

$$R_\beta = \begin{pmatrix} \cos\beta & 0 & -\sin\beta \\ 0 & 1 & 0 \\ \sin\beta & 0 & \cos\beta \end{pmatrix} \quad (2)$$

Point P rotates counterclockwise around the z-axis, and the rotation matrix obtained by the rotation angle β is:

$$R_\gamma = \begin{pmatrix} \cos\gamma & -\sin\gamma & 0 \\ \sin\gamma & \cos\gamma & 0 \\ 0 & 0 & 1 \end{pmatrix} \quad (3)$$

Therefore, in Figure 2, point $P\,(x, y, z)$ rotates through the x, y, and z axes in turn to obtain point $P'(x', y', z')$. The coordinate relationship between point P and P' is:

$$\left[x^{'}y^{'}z^{'}\right]^{T} = R_{\alpha}R_{\beta}R_{\gamma}\left[xyz\right]^{T} \tag{4}$$

Denote the above formula $\boldsymbol{R}_{\alpha}\boldsymbol{R}_{\beta}\boldsymbol{R}_{\gamma}$ as $\boldsymbol{R}=\boldsymbol{R}_{\alpha}\boldsymbol{R}_{\beta}\boldsymbol{R}_{\gamma}$, and define R as the spatial rotation matrix of point P, then:

$$R=\begin{pmatrix}1 & 0 & 0\\ 0 & \cos\alpha & \sin\alpha\\ 0 & -\sin\alpha & \cos\alpha\end{pmatrix}\begin{pmatrix}\cos\beta & 0 & -\sin\beta\\ 0 & 1 & 0\\ \sin\beta & 0 & \cos\beta\end{pmatrix}\begin{pmatrix}\cos\gamma & -\sin\gamma & 0\\ \sin\gamma & \cos\gamma & 0\\ 0 & 0 & 1\end{pmatrix} \tag{5}$$

Simplified:

$$R=\begin{pmatrix}\cos\beta\cos\gamma & -\cos\beta\sin\alpha\sin\beta-\cos\alpha\sin\gamma & -\cos\alpha\cos\gamma\sin\beta+\sin\alpha\sin\gamma\\ \cos\beta\sin\gamma & \cos\alpha\cos\gamma-\sin\alpha\sin\beta\sin\gamma & -\cos\gamma\sin\alpha-\cos\alpha\sin\beta\sin\gamma\\ \sin\beta & \cos\beta\sin\alpha & \cos\alpha\cos\beta\end{pmatrix} \tag{6}$$

The distance from O to P is r:

$$\begin{cases} P^{'}=PR\\ x^{'2}+y^{'2}+z^{'2}=r^{2}\end{cases} \tag{7}$$

The compensation quantity on the △x and △y axis is:

$$\begin{cases}\Delta x=(\cos\beta-1)x-\sin\alpha\sin\beta y\\ \Delta y=(\cos\alpha-1)y\end{cases} \tag{8}$$

According to the above analysis, when controlling the position of the seeding tube, the position coordinates of the seeding tube in the plane is defined. Through the spatial rotation theory, the offset of the position of the seed discharge tube on the x and y planes are obtained. The displacement compensation of x and y axes in the plane can be realized through the servo electric push rod.

- **COMPOSITION AND WORKING PRINCIPLE OF DYNAMIC COMPENSATION SYSTEM**

The dynamic compensation system mainly consists of a six-degree-of-freedom platform, a seeding monomer, a dynamic compensation mechanism, a biaxial tilt sensor and an industrial control computer. The industrial computer uses RS232 to load the excitation signal to the six-degree-of-freedom platform to simulate the position and posture changes of the seeding monomer in field operations. The dual-axis inclination sensor collects the inclination data of the seeding monomer and transmits it to the industrial computer through the CAN bus for processing and analysis. A dynamic compensation mechanism is installed on the seeding monomer, and the dynamic compensation mechanism completes dynamic compensation through servo electric push rod and linear displacement sensor. The compensation range of the system was -5 ~ 5 cm.

When the 6DOF platform receives the loaded analog signal through RS232, the field working state was simulated according to the preset waveform. The seed opening of the seeding tube begins to offset the ideal seeding position, and the biaxial tilt sensor detects the deviation angle change of seeding monomer x and y axis, which is then transmitted to the control system through the CAN bus. The control system adopts the fuzzy PID control servo electric push rod to push the seed row pipe compensation, and the push rod displacement sensor detects whether the seeding tube reaches the predetermined position until the dynamic compensation of the seeding position is completed.

The dynamic compensation mechanism is composed of four parts: the main frame of supplementary seed, the longitudinal compensation unit, the transverse compensation unit and seeding end unit. The vertical and horizontal two-way movement is free superposition without any interference and can operate freely at the same time.

The longitudinal compensation unit by the longitudinal slider, longitudinal guide rails, longitudinal servo electric putter, longitudinal linear displacement sensor and longitudinal slide frame. When the longitudinal servo electric putter stretches or shrinks, the longitudinal slider sliding on the longitudinal guide rail drives the longitudinal slide frame to realize synchronous action. At the same time, the longitudinal linear displacement sensor is lengthened or shortened to realize position measurement.

As shown in Figure 3, the structure of the transverse compensation unit and the longitudinal compensation unit is the same as the motion mode.

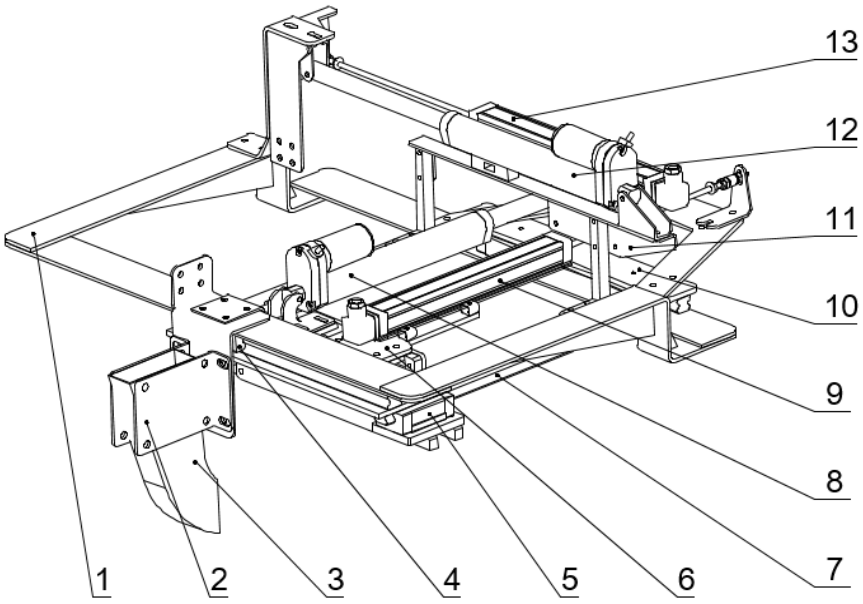

Fig. 3- Structure of dynamic compensation mechanism

1. Transverse slide frame; 2. Seed metering tube support; 3. Seed metering tube; 4. Transverse slider; 5. Longitudinal slider; 6. Compensation main frame; 7. Longitudinal guide rail; 8. Longitudinal servo electric push rod; 9. Longitudinal linear displacement sensor; 10. Transverse guide rail; 11. Longitudinal sliding frame; 12. Lateral servo electric push rod; 13. Transverse linear displacement sensor

FUZZY PID CONTROL

The seeding position compensation system is mainly composed of 2 servo electric push rods to realize offset compensation. The servo electric push rod is driven by servo motor (Panasonic, model MSMF02V2M, rated speed 3000 r/min, rated power 200W).

In the whole system, the dynamic equation and the electrical equation are:

$$\begin{cases} U = E + IR_1 + L_1\dfrac{dl}{dt} = K_1\dfrac{d\theta_1}{dt} + IR_1 + L_1\dfrac{dl}{dt} \\ T = K_2 I \\ T = T_1 + T_2 + T_3 + T_4 \\ T_1 = J_1\dfrac{d\omega}{dt} \\ T_2 = b_1\omega = K(\theta_2 - \theta_1) \\ T_3 = J_2\dfrac{d\omega}{dt} \\ T_4 = b_2\omega = K(\theta_3 - \theta_2) \\ Z = \theta_3 R \end{cases} \quad (9)$$

Where:

U is the armature voltage, V; I is the armature current, A; L_1 is the armature inductance, H;

R_1 - the armature resistance, Ω; Z is the displacement of the push rod, cm;

J_1 - the rotor inertia of the motor, kg·m^2; J_2 is the moment of inertia of the lead screw, kg·m^2;

θ_1 - the angle of rotation of the motor, rad; θ_2 is the rotation angle of the motor driven shaft, rad;

θ_3 - the angle of rotation the lead screw, rad; T_4 is the output torque of the lead screw, N·m;

T - the electromagnetic torque, N·m; T_1 is the inertia torque of the motor, N·m;

T_2 - the motor friction torque, N·m; T_3 is the inertia torque of load, N·m;

T_4 - the friction torque of load, N·m; b_1 is the viscous friction coefficient of the motor, N·m·s/rad;

b_2 - the viscous friction coefficient of the load, N·m·s/rad;

E - the counter electromotive force of the motor, V; K_2 is the motor torque coefficient, N·m/A;

K_1 - the reverse electromotive force coefficient of the motor, V·s/rad;·

K - the stiffness coefficient of the transmission shaft, N·m/rad;

ω - angular velocity of the motor, rad/s;

R the expansion displacement of the push rod per unit angle, mm/rad.

Let $\theta = \theta_1 = \theta_2$ $J = J_1 + J_2$, the transfer function from armature voltage to output displacement is:

$$\frac{Z(s)}{U(s)} = \frac{K_2 R}{(L_1 s + R_1) Js + K_2 K_1} \tag{10}$$

The relevant parameters of the motor used in this test are R_1= 1.2, R =1, L_1= 0.001, K_2= 0.6, K_1 =0.029, J=0.01, and the transfer function of the motor can be obtained by substituting into Equation (10):

$$G(s) = \frac{Z(s)}{U(s)} = \frac{60000}{s^2 + 1200s + 1740} \tag{11}$$

The output and input relation of the motor Simulink model can be represented by this transfer function and will be used as the object of fuzzy PID controller correction.

According to the transfer function, the fuzzy PID controller is designed, and the servo motor fuzzy PID simulation model is established, as shown in Figure 4.

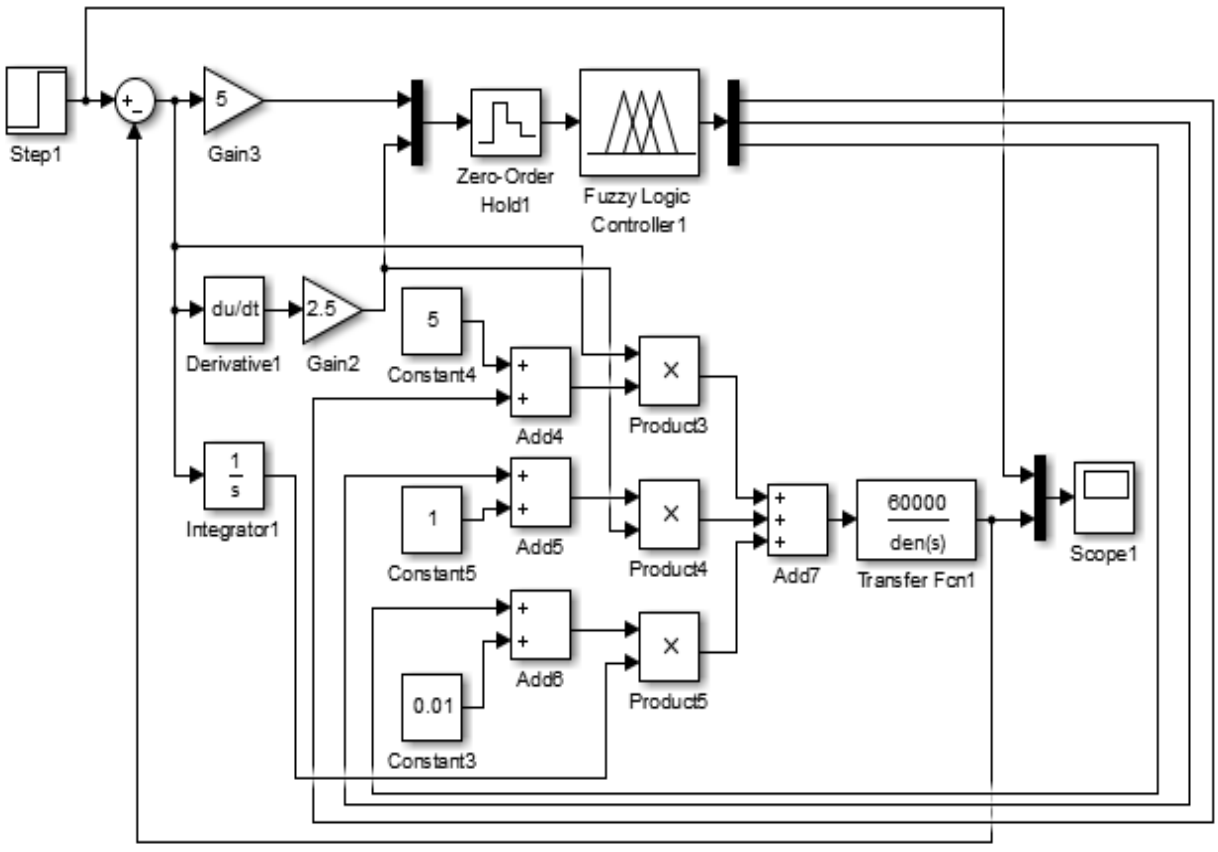

Fig. 4 - Fuzzy PID Simulation Model

RESULTS

To test the dynamic performance of the control system, a step signal with amplitude of 1 is input in the simulation model, and the system dynamic response results are displayed in the Scope oscilloscope. The step response diagram obtained by the Matlab drawing tool is shown in Figure 5. The response time of step response curve of fuzzy PID controller is 0.035 s, and the system curve is stable.

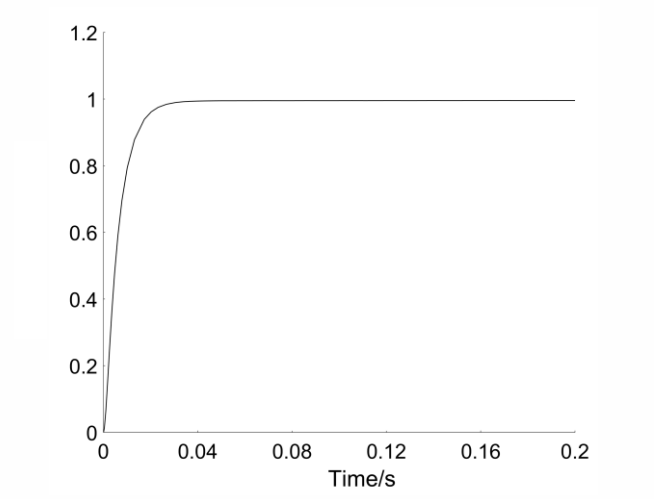

Fig. 5 - Step response curve of fuzzy PID control

In order to study the influence of different factors on the seed dropping position, a three-factor and three-level seed dropping stability test was carried out for three factors: the rotation speed of the seed metering device, the position of the seeding tube and the tilt angle of the seed metering device, to determine the level of each factor based on the single-factor test results. As shown in Table 2, each group was tested 50 times, repeated 3 times, and the position after the corn seed fell was recorded as (x, y), to calculate the variation coefficient of the longitudinal grain spacing y1 and the transverse coefficient of variation y2. The sowing position is negative with respect to the left side of the x-axis and positive on the right side; the inclination of the seed meter is negative with respect to the left side of the xOz plane and positive on the right side.

Table 2

Seed dropping stability test scheme

Coded values	Seed metering device Z_1 / (rad/min)	Seed tube position Z_2 / mm	Inclination angle of seed metering device Z_3 / Degree
- 1	20	- 50	- 10
0	30	0	0
1	40	50	10

The test results are shown in Table 3. A quadratic multiple regression fit was performed on the data in Table 3.

Table3

Test plan and results

The serial number No.	Rotation speed of seed metering device z_1	Location of the seed tube Seed tube position z_2	Inclination angle of seed metering device z_3	Spacing CV of longitudinal grain spacing y_1 / %	CV of transverse grain spacing y_2 / %
1	- 1	- 1	0	11.04	3.92
2	1	- 1	0	14.92	6.56
3	- 1	1	0	11.33	4.21
4	1	1	0	15.05	5.98
5	- 1	0	- 1	10.53	4.08
6	1	0	- 1	14.35	6.82
7	- 1	0	1	10.02	3.78
8	1	0	1	14.22	6.78
9	0	- 1	- 1	25.89	22.07
10	0	1	- 1	24.67	23.45
11	0	- 1	1	23.78	23.76
12	0	1	1	25.21	21.03
13	0	0	0	12.05	4.91
14	0	0	0	12.34	5.35
15	0	0	0	13.22	4.78
16	0	0	0	11.65	5.43
17	0	0	0	13.07	4.52

Note: z_1, z_2 and z_3 are the factor coding values.

The regression equation of each factor on the variation coefficient of the longitudinal grain distance is obtained as:

$$y_1 = 12.47 + 1.95z_1 + 0.079z_2 - 0.28z_3 - 0.04z_1z_2 + 0.095z_1z_3 + 0.66z_2z_3 - 8.52z_1^2 + 6.61z_2^2 + 5.81z_3^2 \quad (12)$$

The regression equation of each factor on the variation coefficient of the transverse grain distance is:

$$y_2 = 5 + 1.27z_1 - 0.2z_2 - 0.13z_3 - 0.22z_1z_2 + 0.065z_1z_3 - 1.03z_2z_3 - 8.52z_1^2 + 8.69z_2^2 + 8.89z_3^2 \quad (13)$$

The variance analysis is performed on the test results, as shown in Table 4. According to Table 4, the P value of the simulation model of the variation coefficient of longitudinal and transverse grain spacing is less than 0.01, indicating that the regression model is extremely significant. The P values of the missing fitting terms were 0.9552 and 0.5330, both of which were greater than 0.05, indicating that the regression equation had a high degree of fit and the regression model was stable.

For the coefficient of variation of longitudinal grain spacing, the regression terms z_2, z_3, z_1z_2, z_1z_3 have no significant effects (P>0.05); the regression terms z_1, z_{12}, z_{22} and z_{32} have extremely significant effects (P<0.01), and the regression term z_2z_3 has a significant impact (P<0.05). For the variation coefficient of the transverse grain spacing, the regression terms z_2, z_3, z_1z_2, z_1z_3 have no significant effects (P>0.05), and the regression terms z_1, z_2z_3, z_{12}, z_{22} and z_{32} have extremely significant effects (P<0.01).

Table 4

Variance analysis

Indexes	Source of variance	Sum of squares	Mean square	*F* values	*P* values
y_1	Model	496.28	55.14	200.64	< 0.0001
	z_1	30.50	30.50	110.97	< 0.0001
	z_2	0.050	0.050	0.18	0.6837
	z_3	0.61	0.61	2.22	0.1797
	z_1z_2	0.0064	0.0064	0.023	0.8830
	z_1z_3	0.036	0.036	0.13	0.7277
	z_2z_3	1.76	1.76	6.39	0.0394
	z_1^2	151.29	151.29	550.48	< 0.0001
	z_2^2	184.15	184.15	670.05	< 0.0001
	z_3^2	142.05	142.05	516.85	< 0.0001
	Loss of quasi item	0.14	0.045	0.10	0.9552
	Pure error	1.79	0.45		
	The sum of the	498.21			
y_2	model	945.71	105.08	754.53	< 0.0001
	z_1	12.88	12.88	92.47	< 0.0001
	z_2	0.34	0.34	2.41	0.1642
	z_3	0.14	0.14	1.03	0.3445
	z_1z_2	0.19	0.19	1.36	0.2819
	z_1z_3	0.017	0.017	0.12	0.7378
	z_2z_3	4.22	4.22	30.32	0.0009
	z_1^2	305.75	305.75	2195.46	< 0.0001
	z_2^2	318.04	318.04	2283.67	< 0.0001
	z_3^2	332.65	332.65	2388.64	< 0.0001
	Loss of quasi item	0.38	0.13	0.85	0.5330
	Pure error	0.59	0.15		
	The sum of the squares	946.69			

DISCUSSION

In the control model, sinusoidal wave and square wave signals are input respectively to analyze the tracking characteristics of the fuzzy PID control system of the servo motor, as shown in Figure 6. It can be seen from Figure 6 that the control precision of the dynamic compensation system for the seeding position of the fuzzy PID controller is 99.5%, and the response speed is 17.2 mm/s. The system is stable and meets the design requirements.

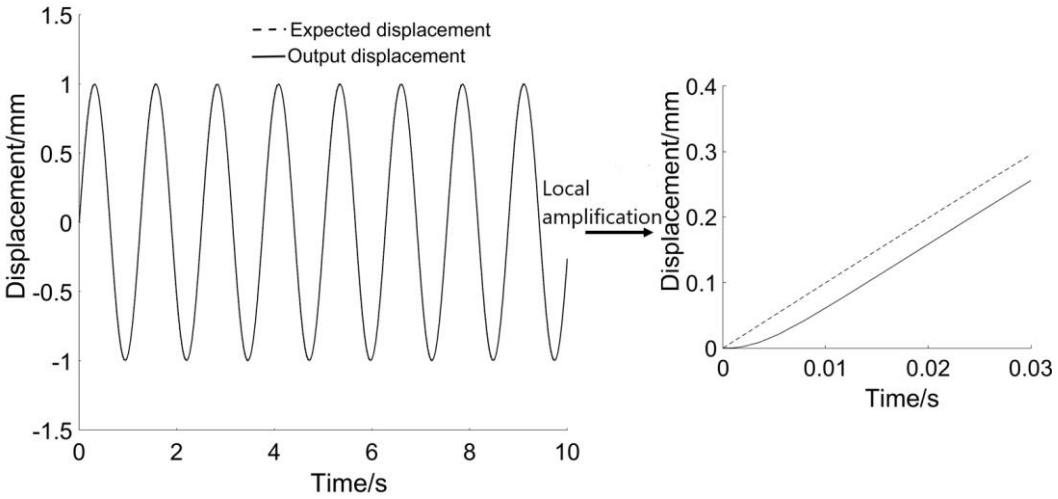

a. Sine wave tracking results

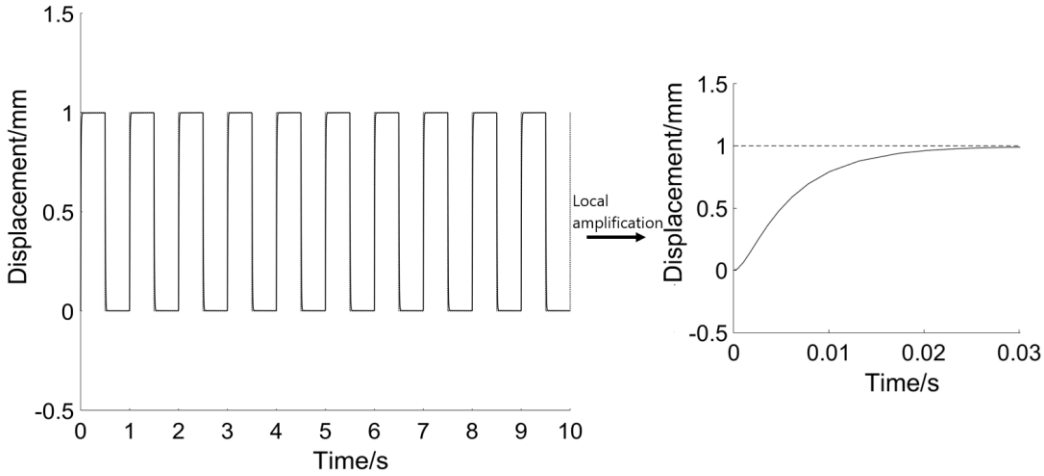

b. Square wave input Tracking results

Fig. 6 - Tracking characteristics of seeding position dynamic compensation system

Figure 7 shows the influence of the interaction between the position of the seeding tube and the angle of the seed metering device on the variation coefficient of the longitudinal and transverse grain distances. As shown in Figure 3, the position of the seeding tube or the inclination angle of the seed metering device individually deviates from the initial position and the variation coefficient of the longitudinal and transverse grain distance increases slowly. For example, when the position of the seed discharge tube deviates from the initial position by 50 mm (z_2 =1), the variation coefficient of the longitudinal grain spacing increases by 6.69%, and that of the transverse grain spacing increases by 8.49%. When the position of the seeding tube and the inclination angle of the seed discharge tube increase at the same time, the variation coefficients of longitudinal grain spacing and the transverse grain spacing increase rapidly, and the upward trend gradually accelerates. For example, when the position of the seeding tube is 50 mm away from the initial position, the angle of the seed metering device is 10°(z_2=1, z_3=1) different from the initial angle. The variation coefficient of the longitudinal grain spacing increased by 12.97 %, and that of the transverse grain spacing increased by 16.29 %.

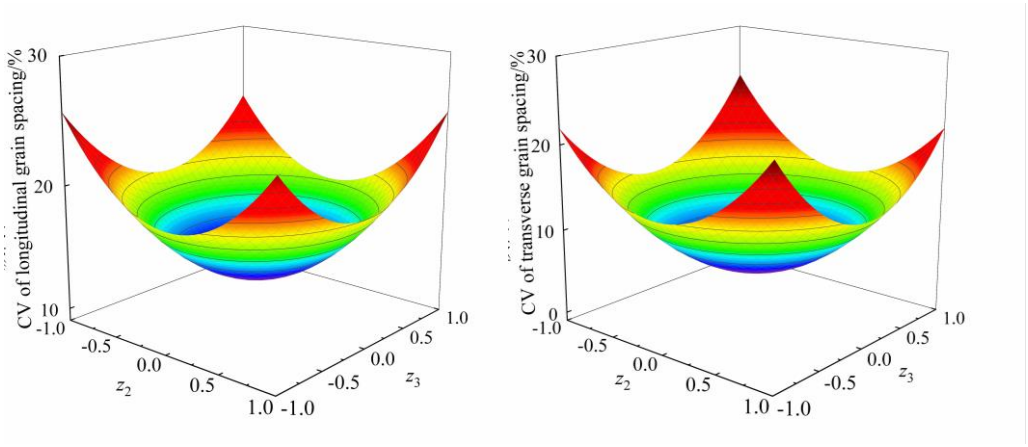

a. $y_1(0, z_2, z_3)$ b. $y_2(0, z_2, z_3)$

Fig. 7 - The interaction between the position of seed metering tube and the inclination angle of metering device on the variation coefficient of longitudinal and transverse grain spacing

From the above analysis, it can be seen that the speed of the seed metering device has a greater impact on the planting position. When only changing the position of the seeding tube or the inclination angle of the seed metering device, it has no effect on the seeding position. When the position of the seeding tube and the inclination angle of the seed metering device change at the same time, the seeding position will change.

CONCLUSIONS

1) High-speed photography was used to test and analyze the seed falling trajectory of the seeding monomer. When the speed of the seed metering device was constant, the angle of the seed metering device and the position of the seeding tube changed at the same time. This would lead to a sharp increase in the variation coefficient of the seed distance and deteriorate the seeding performance.

2) A dynamic compensation system for the seeding position based on PID control was designed. The double-axis angle sensor was used to detect the angle change of the seeding unit, and the offset that should be compensated by the servo electric push rod was calculated through the theory of space rotation. Based on the fuzzy PID, the seeding position was controlled. The electric actuator was dynamically compensated, and the response time of the control system was 0.035 s.

3) The bench test results showed that when the disturbance signal was added, the dynamic compensation function was used by the machine. When there was no dynamic compensation function, the variation coefficient of sowing grain spacing decreased by an average of 6.94%, and that of the transverse grain spacing decreased by an average of 9.16%.

ACKNOWLEDGEMENT

This work was supported by the National Key Research and Development Program of China Subproject (No. 2021YFD2000705), National Natural Science Foundation of China (Grant No. 11626187).

REFERENCES

[1] Ahmad, F., Adeel, M., Qiu, B. J., Ma, J. (2021). Sowing uniformity of bed-type pneumatic maize planter at various seedbed preparation levels and machine travel speeds. *International Journal of Agricultural and Biological Engineering*, Vol. 14(1), pp. 165–171.

[2] Chen, J. L., YAN, R. Z., Chen, B. B. (2018). Research on Grinding Machine Servo Motor Velocity Control of Fuzzy-PID (基于模糊 PID 的磨削机床伺服电机控制研究). *Modular Machine Tool & Automatic Manufacturing Technique*, Vol. 11, pp. 51-53. Shenyang/China.

[3] Huang, D. Y., Zhu, L. T., Jia, H. L., Yu, T. T., Yan, J. (2016). Remote monitoring system for corn seeding quality based on GPS and GPRS (基于 GPS 和 GPRS 的远程玉米排种质量监测系统). *Transactions of the Chinese Society of Agricultural Engineering*, Vol. 32, pp. 162-168(7). Jilin/China.

[4] Huang J. L. (2015). Effect of Precision Sowing and Traditional Sowing on the Growth and Income of Corn (精量播种与传统播种对玉米生长发育及收益的影响). *Journal of Anhui Agricultural Sciences*, Vol. 5, pp. 29-31. Shandong/China.

[5] Ji, J. T., Sang, Y. Y., He, Z. T., Jin, X., Wang, S. S. (2021). Designing an intelligent monitoring system for corn seeding by machine vision and Genetic Algorithm-optimized Back Propagation algorithm under precision positioning. *PloS one*, Jul 15; Vol. 16(7):e0254544.

[6] Joseph, G. L., Mike, R. (2004). Corn response to within row plant spacing variation. *Agronomy Journal*, Vol. 96(5), pp. 1464-1468.

[7] Karimi, H., Navid, H., Besharati, B., Eskandarib, I. (2019). Assessing an infrared-based seed drill monitoring system under field operating conditions. *Computers and Electronics in Agriculture*, Vol. 162, pp. 543-551.

[8] Liu, X. (2013). Research on Mechanized Maize Precision Sowing (玉米精量播种机械化技术研究). *Agricultural Science & Technology and Equipment*, Vol. 1, pp. 66-67. Liaoning/China.

[9] Liu, Y. T., Xu, Y. Y., Wang, Y. X., Yang, H. Y., Gao, P., Wang, J. H. (2017). Effect of Precision Sowing on Growth and Economic Benefit of Maize (精量穴播对玉米生长发育及经济效益的影响). *Heilongjiang Agricultural Science,* Vol. 4, pp. 12-15. Heilongjiang/China.

[10] Moore, S. H. (1991). Uniformity of plant spacing effect on soybean population parameters. *Crop Science*, Vol. 31(4), pp. 1049-1051.

[11] Poncet, A., Fulton, J., McDonald, T., Knappenberger, T., Shaw, J., Bridges R. W., (2018). Effect of Heterogeneous Field Conditions on Corn Seeding Depth Accuracy and Uniformity. *Applied Engineering in Agriculture*, Vol. 34, pp. 819-830.

[12] Precision Planting LLC. (2016). Improve planter performance where it counts - in the meter [EB/OL]. *PM PRECISION AG,* 2016-10-4[2016-10-4].

[13] Sivarajan, S., Maharlooei, M., Bajwa, S. G., Nowatzki, J. (2018). Impact of soil compaction due to wheel traffic on corn and soybean growth, development and yield. *Soil & Tillage Research,* Vol. 175, pp. 234-243.

[14] Wiggans. R. G. (1939). The influence of space and arrangement on the production of soybean plants. *Agronomy Journal,* Vol. 31, pp. 314-321.

[15] Xia, L., Wang, X., Geng, D., Zhang, Q. (2011). Performance Monitoring System for Precision Planter Based on MSP430-CT171. In: Li, D., Liu, Y., Chen, Y. (eds) Computer and Computing Technologies in Agriculture IV. CCTA 2010. *IFIP Advances in Information and Communication Technology*, Vol. 345, Springer, Berlin, Heidelberg.

[16] Xie, C. J., Yang, L., Zhang, D. X., Cui, T., Zhang, K. L. (2021). Seeding parameter monitoring method based on laser sensors (基于激光传感器的播种参数监测方法). *Transactions of the Chinese Society of Agricultural Engineering (Transactions of the CSAE),* Vol. 37, pp. 140-146.

[17] Yang, Y.G., Zhang, W., Yang, G. (2015). Mathematical Models for Controlling Wetted Soil Masses Forming under the Practice of Water Added Corn seeding. *Proceedings of 2015 International Conference on Computer Information Systems and Industrial Applications (CISIA2015)*. pp. 773-776.

[18] Yazgi, A. (2016). Effect of seed tubes on corn planter performance. *Applied Engineering in Agriculture*, Vol. 32, pp. 783-790.

[19] Yin, Y. Q. (2014). On the Development of Precision Seeder Intelligent Monitoring System Controlled by Single-Chip Microcomputer. *Applied Mechanics and Materials*, Vol. 3372(1230), pp. 130-134.

[20] Zhao, S., Chen, J., Wang, J., Yang, C. (2018). Design and Experiment on V-groove Dialing Round Type Guiding-seed Device (精量播种机 V 型凹槽拨轮式导种部件设计与试验). *Transactions of the Chinese Society for Agricultural Machinery*, Vol. 49(6), pp.146-158.